ISSN 1063-7834, Physics of the Solid State, 2018, Vol. 60, No. 9, pp. 1839–1843. © Pleiades Publishing, Ltd., 2018.

IMPURITY CENTERS

Electron Paramagnetic Resonance of Cr^{3+} Ions in Single Crystals of Yttrium Aluminum Borate $YAl_3(BO_3)_4$[1]

A. Vorotynov[a, *], Ya. Shiyan[a], I. Gudim[a], L. Bezmaternykh[a], and O. Vorotynova[b]

[a] *Kirensky Institute of Physics, Federal Research Center KSC SB RAS, Krasnoyarsk, Russia*

[b] *Siberian Federal University, Krasnoyarsk, Russia*

** e-mail: sasa@iph.krasn.ru*

Received March 21, 2018

Abstract—Single crystal of yttrium aluminum borate $YAl_3(BO_3)_4$ doped with chromium ions (1 at %) was studied using electron paramagnetic resonance spectroscopy. It is shown that chromium ions introduced into the sample occupy yttrium ion sites in the crystal structure. The parameters of the spin Hamiltonian of Cr^{3+} ions in the $YAl_3(BO_3)_4$ matrix are determined at different temperatures. The sign of the fine structure parameter D allows the conclusion that the chromium ions in $YA1_3(BO_3)_4$ single crystals have an easy-plane anisotropy.

DOI: 10.1134/S1063783418090354

1. INTRODUCTION

Crystals with magnetic subsystems formed by ions of different types exhibit remarkable magnetic properties. These properties are especially pronounced in rare-earth magnetic materials in which 4*f* ions of rare-earth metals interact with *3d* transition metal ions. The majority of rare-earth metal ions are characterized by a strong anisotropy, and the magnetic anisotropy of the crystals formed by these ions, as a rule, is determined by the competition of anisotropic interactions between the rare-earth and transition metal ions. Among the aforementioned crystals, there exists a class of borates with the structure of the natural mineral huntite $CaMg_3(CO_3)_4$. These compounds are of considerable interest not only in terms of their magnetic properties but also as multifunctional materials that are especially promising for use in constructing instruments due to their high thermal and chemical stabilities. The general formula for borates of this class is written as $AMe_3(BO_3)_4$, where A is a rare-earth metal and Me is a trivalent metal (Al, Ga, Cr, Fe, Sc) [1, 2]. Among them, aluminum borates $AA1_3(BO_3)_4$ have attracted the particular attention of researchers owing to their luminescence properties and possible application in laser technology.

Crystals of yttrium aluminum borate $YA1_3(BO_3)_4$ are characterized by a high hardness, nonhygroscopicity, and chemical stability. As was already mentioned, yttrium aluminum borate crystals have a huntite structure with space group $R32$ [3]. It is worth noting that, in the crystal structure of the $YA1_3(BO_3)_4$ borate, the Y^{3+} ions can be easily replaced by ions of other rare-earth metals, such as Nd^{3+}, Ho^{3+}, Er^{3+}, and Yb^{3+} ions. Moreover, it is known that $YA1_3(BO_3)_4$ borates doped with rare-earth metal ions are promising materials for use in laser engineering [4–6].

In this work, single crystals of the $YA1_3(BO_3)_4$ borate doped with chromium ions were studied using electron paramagnetic resonance spectroscopy.

2. SAMPLE SYNTHESIS AND DESCRIPTION OF THE CRYSTAL STRUCTURE

Trigonal single crystals of the $YAl_3(BO_3)_4$ borate doped with chromium ions were grown using the solution melt method. The initial solution melt used for synthesizing our samples is characterized by a wide range of stability of the high-temperature trigonal phase of the $YAl_3(BO_3)_4$ borate. We chose the $[Bi_2Mo_3O_{12} + pLi_2MoO_4 + qB_2O_3]$ fluxes with $n = 14$, $p = 0.75$, and $q = 2.5$ to grow $Y_{1-x}Cr_xAl_3(BO_3)_4$ ($x = 0.2$). The crystallization parameters for these fluxes were almost the same: specifically, the saturation temperature $T_{sat} \sim 965$°C, the concentration dependence of the saturation temperature $dT_{sat}/dn = (12–15)$°C/wt %, the width of the metastable zone ~20°C, and the crystallization range of $Y_{1-x}Cr_xAl_3(BO_3)_4$ near ~100°C. At an acceptable flux viscosity and a flux density not higher than the crystal density ($\rho_f < \rho_{cr}$), stable crystal growth was provided near the flux surface.

In each case, the flux with a total mass of 100 g was prepared in a cylindrical platinum crucible

[1] The article is published in the original.

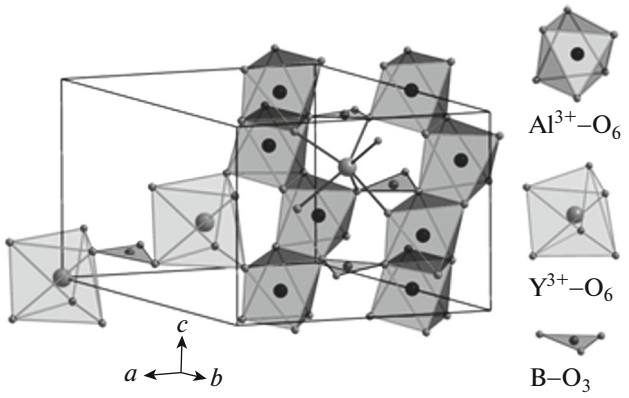

Fig. 1. Crystal structure of yttrium aluminum borate $YAl_3(BO_3)_4$. Not all atoms in the unit cell are shown. The unit cell parameters are as follows: a = 9.295(3) Å, c = 7.243(2) Å, Z = 3, and space group $R32$.

(D = 60 mm, H = 60 mm) by successive alloying of (Bi_2O_3 + MoO_3), B_2O_3, (Y_2O_3 + Al_2O_3 + Cr_2O_3), and (Li_2CO_3 + MoO_3) oxides at T = 1050–1100°C. Then the crucible with the prepared flux was placed in a crystallization furnace with a temperature field whose vertical component at T = 1000°C decreased with a gradient of 1–2°C with increasing distance from the crucible bottom.

After determining T_{sat} and superheating the flux at T = 1050°C for 2–4 h, the carrier was suspended above the flux and the temperature in the furnace decreased to $T = T_{sat}$ + 7°C. Then the carrier with seeds was immersed into the flux to a depth of 15–20 mm and reverse rotation (with a period of 1 min) at a rate of 30 rpm was switched on. After 15 min, the temperature decreased to the starting value, $T = T_{sat} - 7$°C, which corresponds to the middle of the metastable zone. Furthermore, the flux temperature gradually decreased at a programmable set rising rate (1–3°C/day), corresponding to crystal growth at a rate of no more than 1 mm/day. After the end of the growth process, the carrier was lifted above the flux and cooled to room temperature with the furnace supply switched off. The chromium concentration was estimated by placing reagents in the charge as 1 at %.

The main elements of the crystal structure of the yttrium aluminum borate under investigation are schematically shown in Fig. 1.

In the crystal structure of the $YAl_3(BO_3)_4$ borate, the yttrium ions are surrounded by six oxygen ions forming a trigonal bipyramid with symmetry 3*a* (32). The aluminum ions are located in distorted octahedra composed of oxygen ions with symmetry 9*d* (2). The nearest neighbor Y^{3+}–Y^{3+} and Al^{3+}–Al^{3+} ions distances are equal to 5.88 and 3.04 Å respectively.

The superexchange interaction between Y^{3+}–Y^{3+} sites can be realized via B–O_3 group and is considered negligible. The superexchange interaction between aluminum ions sites is realized via two common oxygen ions.

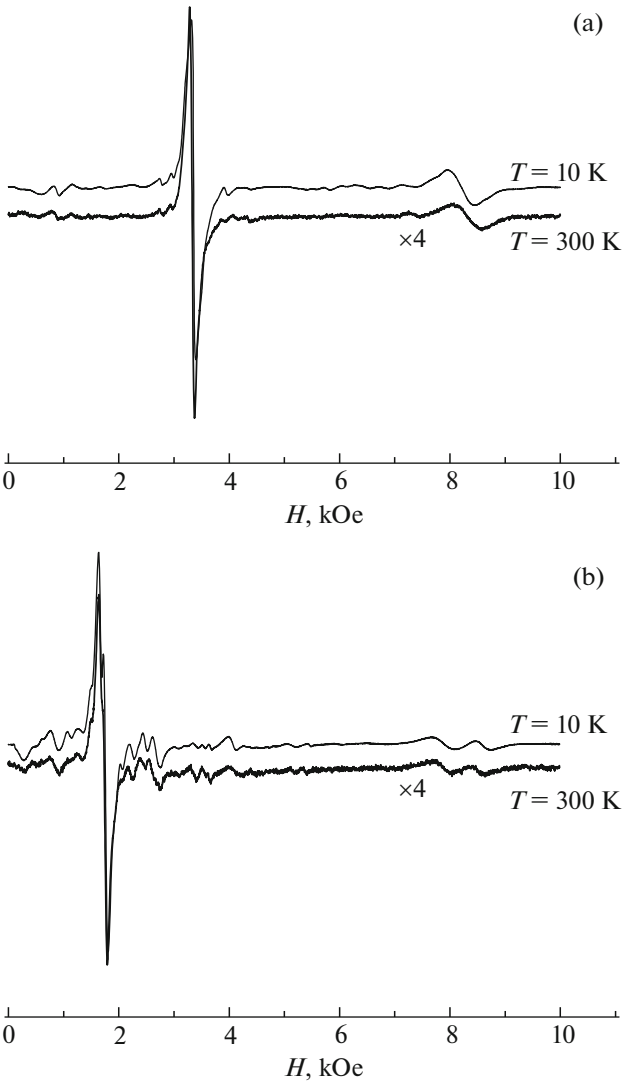

Fig. 2. Typical spectra of Cr^{3+} ions in $YAl_3(BO_3)_4$ for external magnetic field parallel (a) and in basal plane (b) of the crystal.

3. EXPERIMENTAL TECHNIQUE AND RESULTS

The electron paramagnetic resonance spectra of the $YAl_3(BO_3)_4$ single crystal doped with Cr^{3+} ions were recorded on an Bruker EPR spectrometer Elexsys E580 operating at X-band. The measurements were performed at temperatures 300 and 10 K in magnetic fields of up to 10 kOe for different orientations of the single crystal with respect to the external magnetic field.

Figure 2 shows a typical spectrum of the electron paramagnetic resonance in magnetic fields applied

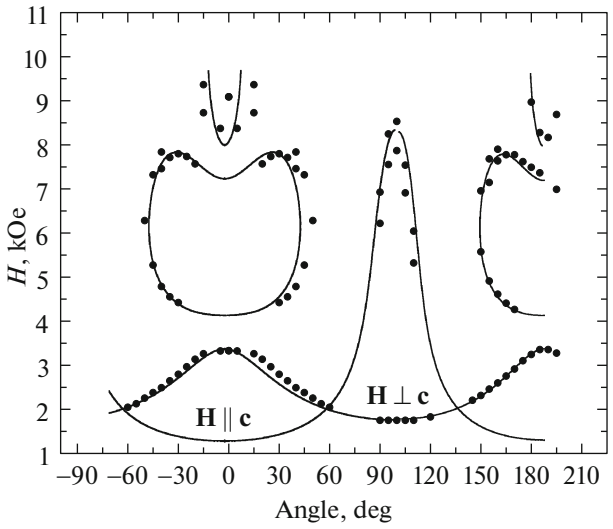

Fig. 3. Angular dependence of the resonance lines of Cr^{3+} ions in $YAl_3(BO_3)_4$ in plane containing *c*-axis of the crystal at room temperature. Closed dots experiment, solid line—fitting curve (see text below).

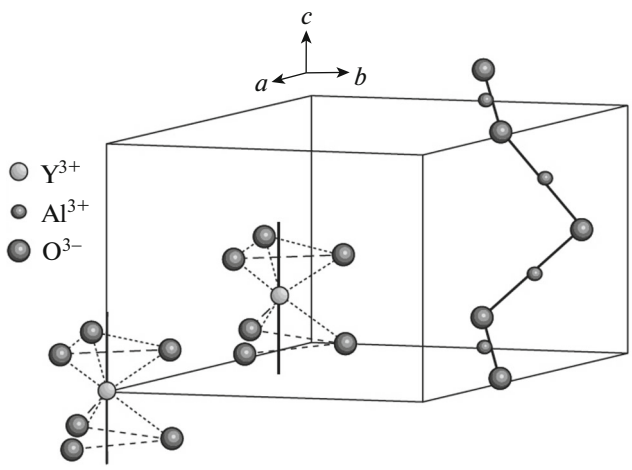

Fig. 4. Positions of the local quantization axes (solid lines) for ions at the yttrium and aluminum sites.

parallel and normal to the trigonal axis *c* of the single crystal.

The spectra mainly consist from one line with strong intensity in the region of 1800–2700 Oe (with linewidth $\Delta H_{pp} \sim 100$ Oe) and the second line with low intensity in the region of 8000 Oe (with linewidth $\Delta H_{pp} \sim 500$ Oe) and are typical for single ion spectra. The remarkable splitting of both resonance lines is observed for magnetic field applied normal to *c*-axis of the crystal (especially for high field region) see Fig. 2.

Figure 3 shows the angular dependence of these lines at different orientation of the external magnetic field with respect to the crystal axis.

In basal plane of the crystal, the angular dependence of the resonance fields of the lines is weak and almost isotropic (see text below).

4. DISCUSSION

First of all, it is necessary to ascertain in what sites (Y^{3+} or Al^{3+}) of the crystal structure the doping chromium ions are situated. As it was mentioned above, the local symmetry of the Y^{3+} and Al $^{3+}$ ions differs from each other. The local symmetry of the Y^{3+} ions is 32 and it means that there is one triad axis along *c*-axis of the crystal and three twofold axes in basal plane (*ab*) of the crystal. The trigonal bipyramid from oxygen ions with such symmetry assumes the presence of the local quantization axis along *c*-axis of the crystal for the Y^{3+} ion site. From this point of view, all Y^{3+} sites are magnetically equivalent to each other. In contrast to this, the local symmetry of the Al^{3+} ions is 2 and assumes the existence of only one twofold axis along one of the *a*, *b*-axis and between them in basal plane (*ab*) for different Al^{3+} ion situated along *c*-axis of the crystal. Moreover, the most elongated axes of the distorted oxygen ions octahedra around Al^{3+} site (defining the quantization axes) forms zigzag chain along *c*-axis of the crystal. So, it is obvious that Al^{3+} sites are not magnetically equivalent to each other.

The local quantization axes for Y^{3+} and Al^{3+} sites are presented in Fig. 4.

From the foregoing it follows that if doping Cr^{3+} ions occupied Al^{3+} sites the significant splitting of the resonance lines will be observed for all orientations of the external magnetic field (both in and out of the basal plane) and three identical resonance spectra will be observed with 60-degrees period. In other case (when doping Cr^{3+} ions occupied Y^{3+} sites), the isotropic spectra must be observed in basal (*ab*) plane and single spectra for planes including *c*-axis of the crystal. The latter case was observed in our experiments. So, we may argue that Cr^{3+} ions are situated in Y^{3+} sites.

Resonance spectra were treated by using axial spin-Hamiltonian

$$H = g_{\parallel}\beta H_z S_z + g_{\perp}\beta(H_x S_s + H_y S_y) + DS_z^2 + E(S_x^2 - S_y^2), \quad (1)$$

where D is axial constant, $E = 1/2(D_x - D_y)$, $g_{\parallel}$ and $g_{\perp}$ are *g*-values for the magnetic field parallel and normal to C_3 axis of the crystal, β is Bohr magneton. Fitting of the experimental spectra were carried out with XSophe program [7].

The calculated angular dependence of the resonance fields in normal to basal plane at room temperature is presented in Fig. 3 by solid line.

In order to understand the resonance lines splitting at external magnetic fields oriented in basal plane (*ab*)

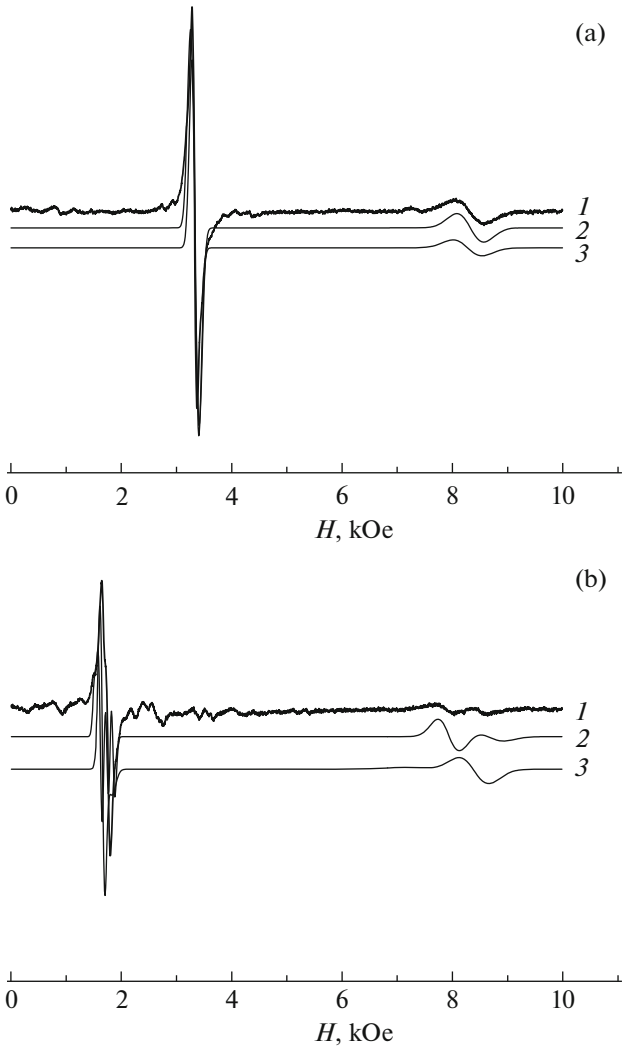

Fig. 5. Experimental and calculated spectra for the external magnetic field parallel (a) and in basal plane (b) of the crystal at room temperatures. (*1*) Experiment, (*2*) calculated spectrum with one nearest Cr^{3+} neighbor, (*3*) calculated spectrum without Cr^{3+} neighbor.

of the crystal the following model was considered. The each yttrium ion has 7 nearest neighbors with distances from 5 to 8 Å. So, we proposed that at Cr^{3+} concentration (~1 at %) at least one nearest neighbor will be Cr^{3+} ion too. Thus, we include in our calculations one nearest neighbor Cr^{3+} at 5.88 Å distance (only dipole-dipole interaction was accounted). It results in calculated spectra, presented in Fig. 5.

As one can see, accounting of one nearest Cr^{3+} neighbor in spectrum calculation agrees well with the experimental spectra for both orientation of the external magnetic field. Figure 6 presents angular dependence of the resonance fields in basal plane of the crystal.

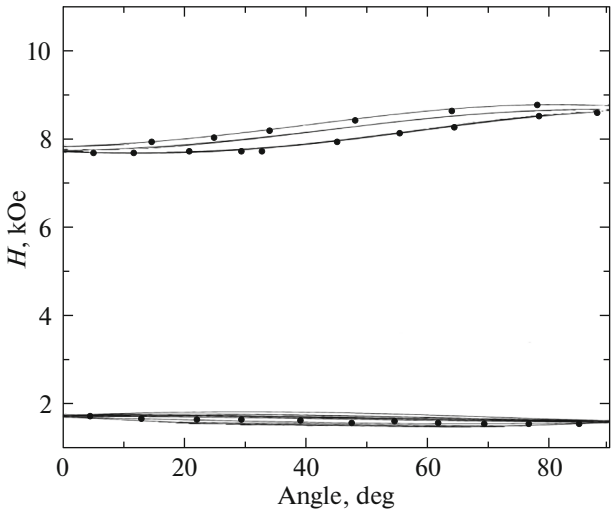

Fig. 6. Angular dependence of the resonance fields in basal plane of the crystal. Closed dots—experiment, solid lines—fitting curves.

The best fitting values of the spin-Hamiltonian (1) at different temperatures are presented in Table 1.

The values of the *g* factors obtained are nearly isotropic and correspond to appropriate values for d^3 ions [8]. The spin-Hamiltonian constant value *D* correlates with those in the earlier investigated compounds Al_2O_3 [9] and $ZnGa_2O_4$ [10, 11].

The sign of the *D* value was determined from the comparison of the intensities of the low and high field resonance lines at temperatures 10 and 300 K.

Let us note, that the *D* value for Cr^{3+} ion obtained in $YAl_3(BO_3)_4$ is greater than for Mn^{2+} ions in this compound investigated by us earlier and has an opposite sign ($D_{Mn^{2+}} \sim -0.073$ cm^{-1}) [12].

It is necessary to note, that earlier in [13] the electron paramagnetic resonance data for Cr^{3+} ion in $YAl_3(BO_3)_4$ were reported. They obtained quit close to our data *D* value ($|D| = 0.52 \pm 0.02$ cm^{-1}) and slightly different *g*-factor values ($g_x \approx g_y \approx g_z = 1.978 \pm 0.005$). The authors [13] argued that Cr^{3+} dopant ions are situated in Al^{3+} octahedral sites contrary to our results. Such conclusion was made for two reasons. First—the angular variation of the EPR resonance lines in basal plane of the crystal (Fig. 3 in [13]) revealed their significant splitting (contrary to our data). Second—because the ionic radius (0.62 Å) of Cr^{3+} is close to

Table 1. Values of the spin-Hamiltonian (1)

T, K	*D*, cm^{-1}	*E*/*D*	$g_\perp$	$g_\parallel$
10	+0.524(3)	0.03(2)	1.938(3)	1.932(5)
300	+0.527(1)	0.025(2)	1.948(1)	1.939(1)

that (0.53 Å) of Al^{3+}. We do not in any way put in doubt the experiential results in [13]. To our mind, such discrepancies may be caused by different growth technique was used. Particularly, usage of $K_2Mo_3O_{10}$ in [13] instead of $Bi_{12}Mo_3O_{12}$ (was used by us) may force Cr^{3+} ions to occupy the Y^{3+} positions. For example, in our previous paper [12] we do not observed any resonance line splitting for Mn ions in basal plane of the crystal in $YAl_3(BO_3)_4$ also.

5. CONCLUSIONS

Electron paramagnetic resonance of Cr^{3+} ions in $YAl_3(BO_3)_4$ single crystal was studied. The symmetry considerations and angular dependencies of the resonance lines unambiguously allow to claim that Cr^{3+} ions occupy Y^{3+} sites in $YAl_3(BO_3)_4$ matrix. It was shown, that resonance properties of Cr^{3+} ions are well described by the axial spin-Hamiltonian. The parameters of the spin-Hamiltonian were determined for temperatures 10 and 300 K. Easy-plane type anisotropy of the Cr^{3+} in $YAl_3(BO_3)_4$ single crystal was established.

REFERENCES

1. G. Blasse and A. Bril, Phys. Status Solidi **20**, 551 (1967).
2. V. I. Chani, M. I. Timoshechkin, K. Inoue, K. Shimamura, and T. Fukuda, Inorg. Mater. **30**, 1466 (1994).
3. N. I. Leonyuk and L. I. Leonyuk, Prog. Cryst. Growth Charact. Mater. **31**, 179 (1995).
4. N. I. Leonyuk, E. B. Koporulina, K. L. Bray, and D. Hansen, J. Cryst. Growth **191**, 767 (1998).
5. A. Brenier, Opt. Commun. **141**, 221 (1997).
6. D. Jaque, J. Capmany, and S. Qarcia, Appl. Phys. Lett. **75**, 325 (1999).
7. M. Griffin, A. Muys, C. Noble, D. Wang, C. Eldershaw, K. E. Gates, K. Burrage, and G. R. Hanson, Mol. Phys. Rep. **26**, 60 (1999).
8. S. A. Altshuler and B. M. Kozyrev, *Electron Paramagnetic Resonance of Compounds of Intermediate Group Elements* (Nauka, Moscow, 1972) [in Russian].
9. M. J. Berggren, G. F. Imbusch, and P. L. Scott, Phys. Rev. **188**, 675 (1969).
10. J. C. M. Henning, J. H. den Boeff, and G. G. P. van Gorkom, Phys. Rev. B **7**, 1825 (1973).
11. G. L. McPherson and Wai-Ming Heung, Solid State Commun. **19**, 53 (1976).
12. A. M. Vorotynov, G. A. Petrakovskii, Ya. G. Shiyan, L. N. Bezmaternykh, V. E. Temerov, A. F. Bovina, and P. Aleshkevych, Phys. Solid State **49**, 463 (2007).
13. J.-P. R. Wells, M. Yamaga, T. P. J. Han, and M. Honda, J. Phys.: Condens. Matter **15**, 539 (2003).